Broadband polarimeter receivers at 30 and 40 GHz for cosmic microwave background measurement

Artal, E., Aja, B., de la Fuente, L., Hoyland, R., Villa, E.

E. Artal, B. Aja, L. de la Fuente, R. Hoyland, E. Villa, "Broadband polarimeter receivers at 30 and 40 GHz for cosmic microwave background measurement," Proc. SPIE 11453, Millimeter, Submillimeter, and Far-Infrared Detectors and Instrumentation for Astronomy X, 1145316 (13 December 2020); doi: 10.1117/12.2561356

SPIE.

Event: SPIE Astronomical Telescopes + Instrumentation, 2020, Online Only

Broadband polarimeter receivers at 30 and 40 GHz for Cosmic Microwave Background measurement

E. Artal[a], B. Aja[a], L. de la Fuente[a], R. Hoyland[b], E. Villa[b]
[a]Dept. Ingeniería de Comunicaciones, Universidad de Cantabria, 39005 Santander, Spain;
[b]Instituto de Astrofísica de Canarias, 38205 La Laguna, Tenerife, Spain

ABSTRACT

Broadband radiometers at 30 and 40 GHz for QUIJOTE radio astronomy experiment are very sensitive receivers to perform scientific sky observations of the Cosmic Microwave Background (CMB). The aim of this experiment is the linear polarization percentage measurement of the received signals. Radiometers have cryogenically cooled Front-End Modules followed by room temperature amplification, correlation and detection modules. Their relative bandwidth is around 30%. There are 30 receivers (pixels) at 30 GHz and 29 receivers at 40 GHz. The radiometer scheme is based on two balanced branches, microwave correlation and direct detection. The manufactured receivers measure Stokes polarization parameters I, Q, and U simultaneously. This paper describes the principle of operation of polarimeter receivers, and present details of manufactured subsystems, integration and test results. Receivers integrate different technologies: waveguides, microstrip, Monolithic Microwave Integrated Circuits (MMIC) and active and passive devices. The receivers are currently under installation in El Teide Observatory, Tenerife (Canary Islands, Spain).

Keywords: CMB receiver, radiometer, polarimeter, broadband receiver, Ka band receiver, Q band receiver, Low Noise Receiver

1. INTRODUCTION

The Thirty and Forty GHz polarimeters for the Q-U-I JOint TEnerife (QUIJOTE) CMB radio astronomy experiment, [1, 2] are broadband very sensitive receivers to perform scientific sky observations of the Cosmic Microwave Background (CMB). The aim of the QUIJOTE experiment is the measurement of the linear polarization percentage of the received waves from the sky. Scientific data will be used for cosmological analysis of the Universe and the indirect detection of gravitational waves. The receivers are radiometers based on cryogenically cooled front-end modules followed by room temperature back-end modules performing amplification, correlation and detection. Relative bandwidth is around 30%. The radiometers scheme is based on two balanced branches and direct detection. Thirty GHz Instrument (TGI) and Forty GHz Instrument (FGI) are multipixel radio telescope receivers composed of about 30 pixels. Each pixel has an individual receiver.

2. TELESCOPES

The QUIJOTE CMB experiment consists of two identical telescopes installed inside a unique enclosure, Figure 1, in El Teide Observatory, Tenerife, Spain. The layout of both telescopes is based on an altazimuth mount supporting a primary reflector and a secondary reflector oriented as an offset Gregorian Dragon scheme.[3] There are two off-axis parabolic reflectors: primary reflector of 2.25 m and secondary reflector of 1.85 m. Telescope design provides low cross-polarization and a symmetric radiation beam.

The system is under-illuminated to minimize side-lobes and ground spillover. Each telescope is mounted on its own platform that can rotate around the vertical axis at a maximum frequency of 6 rpm (i.e., 36 deg/s). Instruments are located on the telescope focal plane, attached to the rear side, Figure 2, and then they move with the telescope according azimuth and elevation settings. Both telescopes have an unlimited rotation capacity in azimuth axis and a range of movement

[a] Further author information: (send correspondence to E. Artal), email: eduardo.artal@unican.es

Millimeter, Submillimeter, and Far-Infrared Detectors and Instrumentation for Astronomy X,
edited by Jonas Zmuidzinas, Jian-Rong Gao, Proc. of SPIE Vol. 11453, 1145316

between 25° to 95° in elevation axis. An integrated rotary joint transmits fluid, power and signal to the rotary elements. The pointing and tracking accuracies are better than 1.76 arcmin and 44 arcsec, respectively.

Figure 1. QUIJOTE telescopes installed in El Teide Observatory, Tenerife, Spain

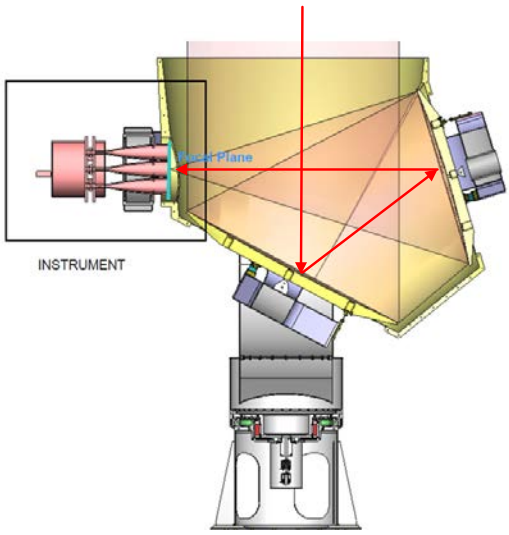

Figure 2. Cross-sectional view of the telescope oriented in zenith position.

3. RECEIVER SCHEMES

The TGI and FGI receivers [4, 5] are polarimeters to obtain three (of four) Stokes parameters (I, Q, U). The Cosmic Microwave Background (CMB) has a very weak linear polarization. The designed receivers measure the Q, U and I Stokes parameters simultaneously. The remaining Stokes parameter is V = 0, because the CMB does not have circular polarization. Stokes parameters are calculated from the incoming signal field components. TGI and FGI have almost identical schemes, with only a difference in the type of 3 dB hybrid couplers in the correlation stage. Block diagrams in Figure 4 show the configuration of each receiver.

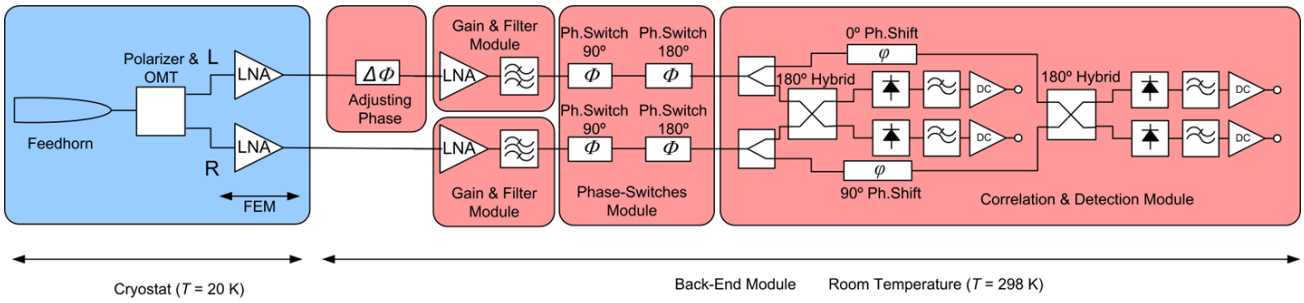

(a)

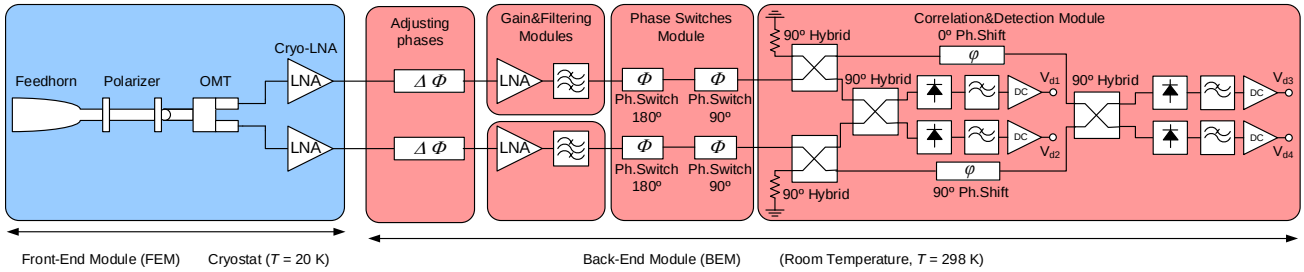

(b)

Figure 3. Block diagrams of the receivers (one pixel): (a) Thirty GHz Instrument, (b) Forty GHz Instrument

Each pixel of a receiver is composed of a cold Front-End Module (FEM) at 20 K, and a room temperature (298 K) Back-End Module (BEM). The cryogenic part is made up of a feedhorn, a polarizer, an Ortho-Mode Transducer (OMT) and two cryogenic low-noise amplifiers (Cryo-LNA). Passive components in the FEM are cryogenically cooled to minimize their contribution to the system noise temperature.

Outside the cryostat, two Gain and Filtering Modules, Phase Switches Module and Correlation and Detection Module operate at room temperature, in which the microwave signal is amplified, filtered, decorrelated by 180º or 90º hybrids and, finally, converted into DC voltages using square-law detectors. These signals are collected by a data acquisition system (DAS). The Phase Switches Modules comprise a four phase-state circuit generating four polarization states. Their performance is crucial in order to obtain the Stokes parameters, minimizing the leakage among them and, at the same time, overcoming the 1/f noise and different systematic errors in the receiver. In front of the BEM, adjusting phases are located to balance the insertion phase between both branches. This adjustment must be done experimentally for each pixel in the integration and verification phase.

The combination of a 90º polarizer and the OMT give two signals at the output of the OMT. Each signal is proportional to the left hand (L) and right hand (R) circularly polarized components of the electric field received by the feedhorn antenna. Two separate branches amplify and filter L and R signals. Ideally, both branches should have identical amplitude and phase responses. A fine adjustment for a balanced phase response in both branches is made by adjusting phase components.

A Correlation-Detection module performs signals decorrelation and direct detection (rectification and filtering of the microwave signal) to low frequency. In order to allow the correction of systematic errors of each receiver, both signals are phase modulated before their correlation. The Phase-Switches Module make this phase modulation in two identical branches, containing 180º and 90º broadband phase-switches. Signal correlation consists basically in addition and subtraction of broadband microwave signals, by a system based on 3 dB/90º or 3 dB/180º hybrid couplers and a fixed 90º phase shifter in a branch.

According to the Phase-Switches state, of the four possible states (0º, 90º, 180º and 270º), the output detected signals from the Correlation-Detection module, are proportional to different combinations of Stokes parameters (Q, U, I), which define the degree of polarization of an electromagnetic wave. The extraction of those Stokes parameters magnitudes, from observations with the instruments, is the experiment main objective.

4. PRINCIPLE OF OPERATION

Stokes parameters are calculated from the incoming signal field components. Using a circular basis of coordinates for the electromagnetic fields:

$$(\hat{l}, \hat{r}) \tag{1}$$

the total electric field received by the feedhorn is a combination of left hand and right hand circular electric fields:

$$\bar{E} = E_l \, \hat{l} + E_r \, \hat{r} \tag{2}$$

The electric field in rectangular coordinates is:

$$\bar{E} = E_x \, \hat{x} + j \, E_y \, \hat{y} \tag{3}$$

where these components can be expressed as

$$E_x = \frac{E_l + E_r}{\sqrt{2}} \quad ; \quad E_y = \frac{E_l - E_r}{\sqrt{2}} \tag{4}$$

The Stokes parameters I, Q and U are obtained from left and right hand circular polarized components of the electric field:

$$\begin{bmatrix} I \\ Q \\ U \end{bmatrix} = \begin{bmatrix} |E_l|^2 + |E_r|^2 \\ 2\, Re(E_l^{\,*}\, E_r) \\ -2\, Im(E_l^{\,*}\, E_r) \end{bmatrix} \tag{5}$$

The combination of a 90º polarizer and the OMT give two signals at the output of the OMT. Each signal is proportional to the electric field components E_l or E_r of the total electric field received by the feedhorn antenna. In Figure 4 there is a sketch of the signals A and B obtained at the output of the assembly feedhorn-polarizer-OMT.

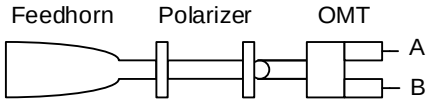

Figure 4. OMT output signals

Simplified block diagrams of TGI and FGI receiver are in Figure 5. Front-End and Back–End amplifiers, filters and diode detectors are not included in block diagrams.

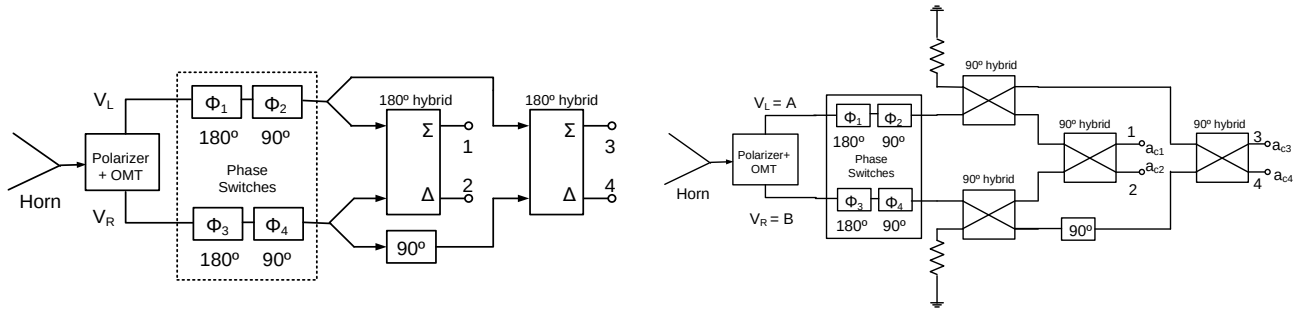

Figure 5. Simplified block diagrams of receivers: (a) Thirty GHz Instrument; (b) Forty GHz Instrument

In the case of FGI, the correlation is based on 3 dB/90º hybrids. The scheme and ports numbers for the 90º hybrid and its S-parameters matrix are shown in Figure 6.

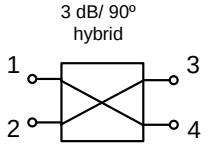

$$[S] = -\frac{1}{\sqrt{2}}\begin{bmatrix} 0 & 0 & j & 1 \\ 0 & 0 & 1 & j \\ j & 1 & 0 & 0 \\ 1 & j & 0 & 0 \end{bmatrix}$$

Figure 6. S-parameter matrix of the 90º hybrids

Assuming as initial state a null phase in the Phase-Switches

$$\emptyset_1 = \emptyset_2 = \emptyset_3 = \emptyset_4 = 0^o \tag{6}$$

the input voltages into the Correlation and Detection Module are A and B. Solving the equations with S-parameters, the final result for the voltages at the outputs in Figure 5(b) are:

$$a_{c1} = \frac{1}{2}(-A + jB) = -\frac{1}{2}(A - jB) \tag{7}$$

$$a_{c2} = \frac{1}{2}(jA - B) = \frac{1}{2}j(A + jB) \tag{8}$$

$$a_{c3} = \frac{1}{2}j(A - B) \tag{9}$$

$$a_{c4} = \frac{1}{2}(A + B) \tag{10}$$

These signals are detected by square-law Schottky diode detectors and amplified by DC amplifiers. The signals at the BEM output are proportional to the squared amplitudes of signals in equations (7) to (10). Discarding the ½ factor, the voltage at the BEM outputs, scheme in Figure 3(b), are as follows:

$$V_{d1} = |A - jB|^2 \tag{11}$$

$$V_{d2} = |A + jB|^2 \tag{12}$$

$$V_{d3} = |A - B|^2 \tag{13}$$

$$V_{d4} = |A + B|^2 \tag{14}$$

From the expression (5) the three Stokes parameters (I, Q, U) can be calculated by substitution of circular polarized electric fields:

$$E_l = A \quad ; \quad E_r = B \tag{15}$$

The Stokes parameters values are obtained as:

$$I \equiv |E_l|^2 + |E_r|^2 \; = \; |A|^2 + |B|^2$$

$$I \equiv V_{d1} + V_{d2} = V_{d3} + V_{d4} = |A + B|^2 + |A - B|^2 = |A + jB|^2 + |A - jB|^2 \tag{16}$$

$$Q \equiv 2\, Re(E_l^{\,*}\, E_r) = 2\, Re(A^*\, B)$$

$$Q \equiv V_{d4} - V_{d3} \; = |A + B|^2 - |A - B|^2 \tag{17}$$

$$U \equiv -2\, Im(E_l^{*}\, E_r) = |A + jB|^2 + |A - jB|^2$$

$$U \equiv V_{d2} - V_{d1} = |A + jB|^2 - |A - jB|^2 \tag{18}$$

Stokes parameters are normalised values ranging from -1 to +1. The intensity I is always equal to +1, then the expressions (16) to (18) should be normalized accordingly.

Introducing the different phase states and assuming that only the upper branch will change its phase, then:

$$\emptyset_T = \emptyset_1 + \emptyset_2\ ;\ \ \emptyset_3 + \emptyset_4 = 0^o \tag{19}$$

$\emptyset_T$ is the phase difference between both receiver branches. The calculation of output voltages for the different states (0º, 90º, 180º and 270º) give the results contained in Table 1.

Table 1. Output voltages at different phase states in FGI receivers

$\emptyset_T$	0º	90º	180º	270º
V_{d1}	$\|A - jB\|^2$	$\|A - B\|^2$	$\|A + jB\|^2$	$\|A + B\|^2$
V_{d2}	$\|A + jB\|^2$	$\|A + B\|^2$	$\|A - jB\|^2$	$\|A - B\|^2$
V_{d3}	$\|A - B\|^2$	$\|A + jB\|^2$	$\|A + B\|^2$	$\|A - jB\|^2$
V_{d4}	$\|A + B\|^2$	$\|A - jB\|^2$	$\|A - B\|^2$	$\|A + jB\|^2$

Finally, the Stokes parameters calculation is made in a similar way as it is done in equations (16), (17) and (18) for the different phase states. Stokes parameters in terms of output detected voltages are in Table 2.

Making a similar analysis for the TGI receiver, with correlation based on 3 dB/180º hybrids, Figure 5(a), the Stokes parameters, in terms of output detected voltages, for each phase state are shown in Table 3.

Table 2. Stokes parameters at different phase states in FGI receivers

$\emptyset_T$	I	Q	U
0º	$V_{d1} + V_{d2} = V_{d3} + V_{d4}$	$V_{d4} - V_{d3}$	$V_{d2} - V_{d1}$
90º	$V_{d1} + V_{d2} = V_{d3} + V_{d4}$	$V_{d2} - V_{d1}$	$V_{d3} - V_{d4}$
180º	$V_{d1} + V_{d2} = V_{d3} + V_{d4}$	$V_{d3} - V_{d4}$	$V_{d1} - V_{d2}$
270º	$V_{d1} + V_{d2} = V_{d3} + V_{d4}$	$V_{d1} - V_{d2}$	$V_{d4} - V_{d3}$

Table 3. Stokes parameters at different phase states in TGI receivers

$\emptyset_T$	I	Q	U
0º	$V_{d1} + V_{d2} = V_{d3} + V_{d4}$	$V_{d1} - V_{d2}$	$V_{d3} - V_{d4}$
90º	$V_{d1} + V_{d2} = V_{d3} + V_{d4}$	$V_{d3} - V_{d4}$	$V_{d2} - V_{d1}$
180º	$V_{d1} + V_{d2} = V_{d3} + V_{d4}$	$V_{d2} - V_{d1}$	$V_{d4} - V_{d3}$
270º	$V_{d1} + V_{d2} = V_{d3} + V_{d4}$	$V_{d4} - V_{d3}$	$V_{d1} - V_{d2}$

5. POLARIZATION SEPARATION: PASSIVE COMPONENTS

Each receiver is composed of a Front-End Module (FEM), cooled cryogenically, and a Back-End Module (BEM) operated at room temperature. The FEM contains passive waveguide components from the antenna to the input of cryogenic low-noise amplifiers (cryo-LNA): feedhorn, polarizer and OMT. A 3D view of the FEM subsystems of FGI receiver is depicted in Figure 7. In the case of TGI receiver the FEM concept is identical.

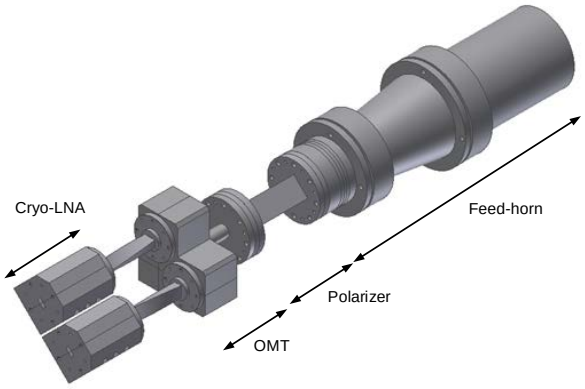

Figure 7. Front-End Module subsystems of FGI receiver

The polarizer is a differential 90º phase shifter for the two orthogonal propagation modes (TE_{10} and TE_{01}) in the square waveguide. The polarizer is rotated 45º in relation to the y-axis of the feed-horn. The constant phase difference, between both modes, is achieved by internal stepped ridges in the square waveguide, placed in its four internal walls. When the electric field at the polarizer input has a linear horizontal or vertical orientation (Figure 8), each orthogonal component propagates along the ridged square waveguide with a different insertion phase. At the polarizer output, field components have 90º phase difference between them.

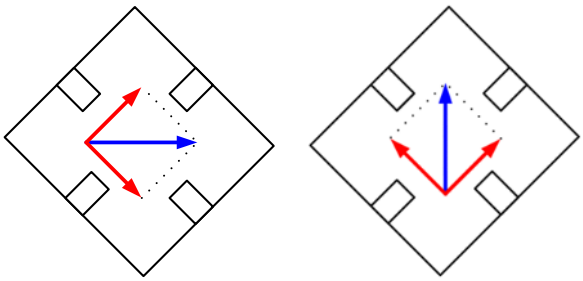

Figure 8. Horizontal (H) and vertical (V) electric field (blue) at polarizer input. Orthogonal TE_{10} and TE_{01} components (red).

The OMT is based on a turnstile junction with an inserted scatterer. Its design consists of a circular waveguide input and two WR22 rectangular waveguide in-phase outputs. The assembly polarizer-OMT (Figure 9) has three physical ports and four electrical ports, since at the polarizer input there are two orthogonal modes. Port numbers for the S-parameters matrix are as follows:

- Port #1: OMT output H
- Port #2: OMT output V
- Port #3: Polarizer input H
- Port #4: Polarizer input V

From simulations, confirmed by experimental tests of the assembly Polarizer-OMT, the ideal S-parameter matrix is:

$$[S] = \frac{1}{\sqrt{2}} \begin{bmatrix} 0 & 0 & 1 & -j \\ 0 & 0 & -j & 1 \\ 1 & -j & 0 & 0 \\ -j & 1 & 0 & 0 \end{bmatrix} \tag{20}$$

The reference phase (0º) is taken for the transmission parameter relating the polarizer input H with the OMT output H. According to (20) with an input horizontal electric field E coming into port #3, the two OMT output signals have the same amplitude but are phase shifted by 90º. The same happens if an input vertical electric field E comes into port #4, then the two OMT output signals have the same amplitude and are phase shifted by 90º.

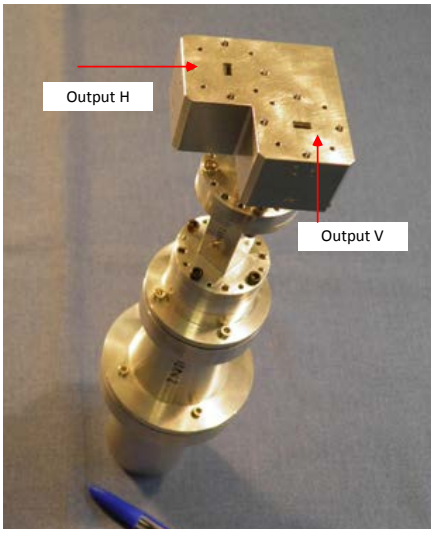

Figure 9. Assembly Feedhorn-Polarizer-OMT of FGI receiver.

6. LOW NOISE AMPLIFIERS

6.1 Thirty GHz Instrument cryogenic LNA

Cryogenic LNA is a two stages low noise amplifier: a first MMIC low noise amplifier on 100 nm MHEMT technology from the Fraunhofer IAF, Freiburg, Germany, and a second MMIC low noise amplifier on 130 nm MHEMT technology from the OMMIC foundry, France. A 5 dB attenuator is between both amplifiers, in order to reduce gain and to assure stability. An internal view of this amplifier and an external view of three units are in Figure 10.

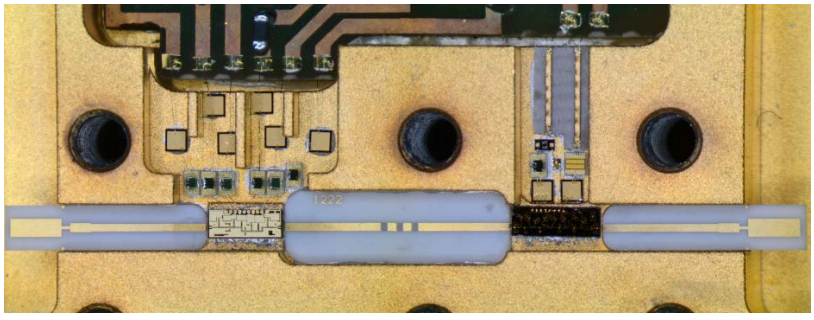

(a)

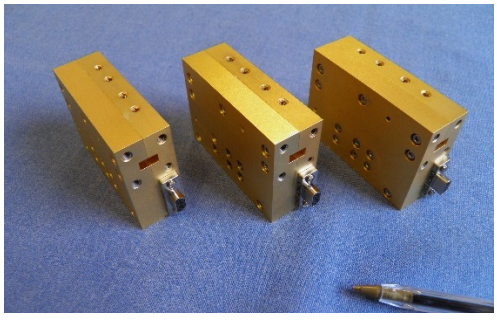

(b)

Figure 10. Cryogenic low noise amplifier of TGI receiver: (a) internal view, (b) external view of three units.

DC bias circuitry warrants out of band stability and protection against over-voltages. All the DC circuitry as well as the RF part are included in the same box with a WR-28 waveguide input and output connections. Figure 11 shows in band (26 to 36 GHz) noise temperature and average gain values obtained from 62 tested units at 12 K.

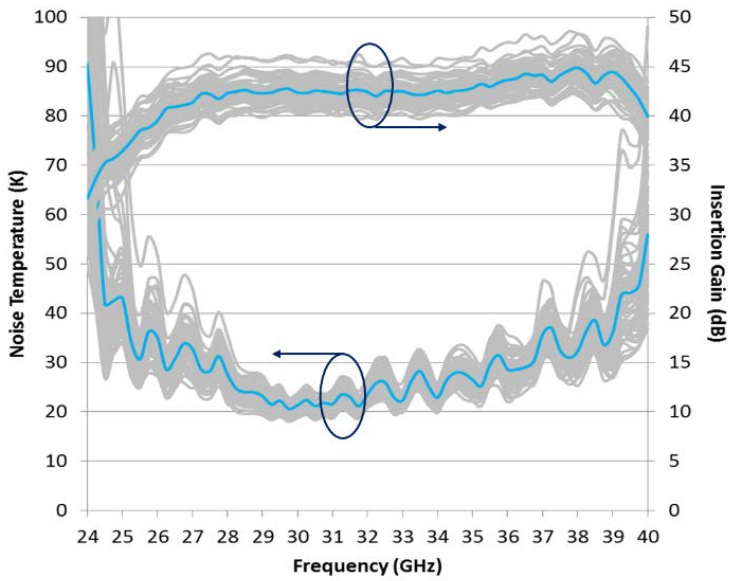

Figure 11. Cryogenic LNA for TGI receiver. Average of 62 tested units at 12 K in 26-36 GHz band.
Noise Temperature ≈ 25 K, Gain ≈ 43 dB.

6.2 Forty GHz Instrument cryogenic LNA

Cryogenic LNA is a two stages low noise amplifier containing two MMIC low-noise amplifiers on 100 nm mHEMT technology from the Fraunhofer IAF (Freiburg, Germany). The MMIC amplifier has four stages with mHEMT transistors having a 4x15 µm gate periphery. An equalizer is placed between both MMIC amplifiers to assure stability and to improve the gain versus frequency slope. A total compensation of the slope could not be achieved because it would have implied a higher noise temperature of the whole module. The RF input and output are through WR-22 waveguide connectors.

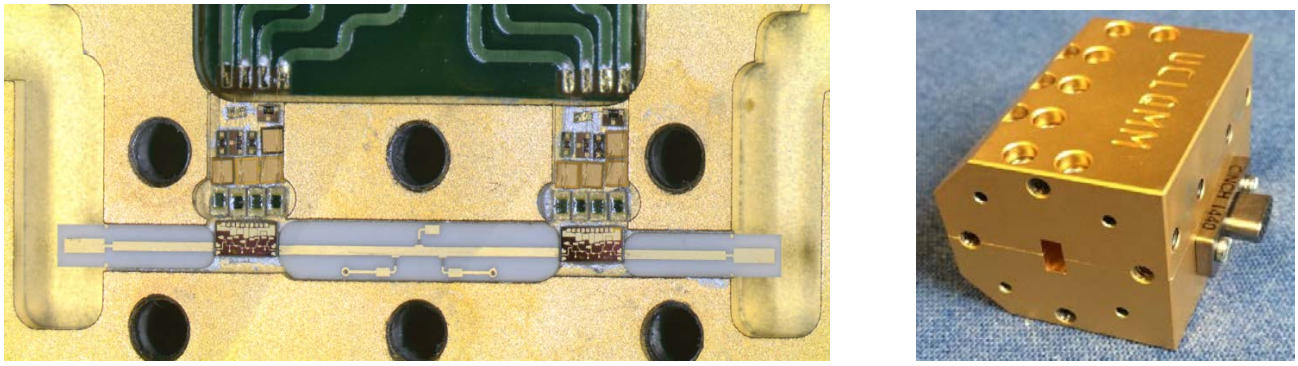

(a) (b)

Figure 12. Cryogenic LNA for FGI receiver: (a) Internal view, (b) External view.

Figure 13 shows in band (35 to 47 GHz) average gain and noise temperature values, obtained from 58 tested units at 18 K.

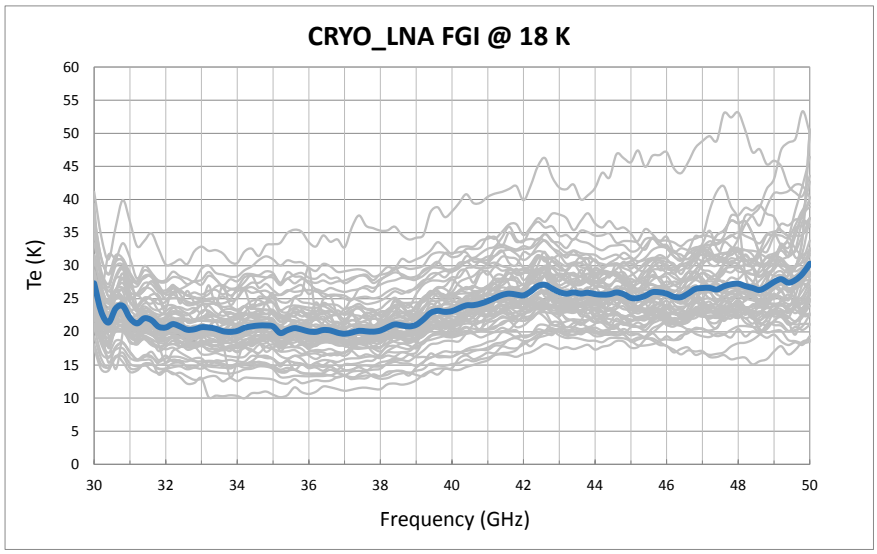

(a)

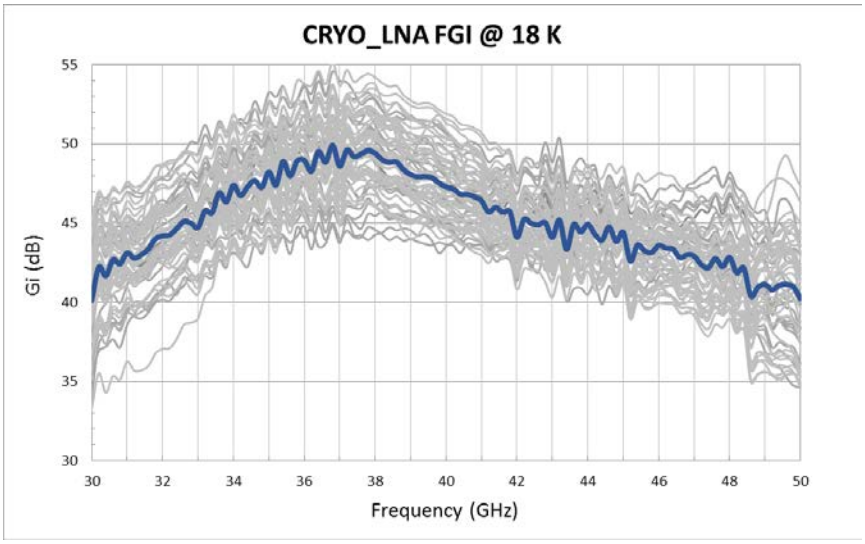

(b)

Figure 13. Cryogenic LNA for FGI receiver. Average of 58 tested units at 18 K in 35-47 GHz band.
(a) Noise Temperature ≈ 23.5 K, (b) Gain ≈ 46.4 dB.

Further signal amplification is done in the Back-End Module at room temperature, Figure 3(b). The Gain and Filtering Module is composed of two cascaded MMIC commercial LNA, with an equalizer in-between and a microstrip filter to define the 35 to 47 GHz bandpass. Its gain is around 30 dB. A detailed view is in Figure 14. This module has a positive gain slope to flatten the amplitude response of the overall receiver.

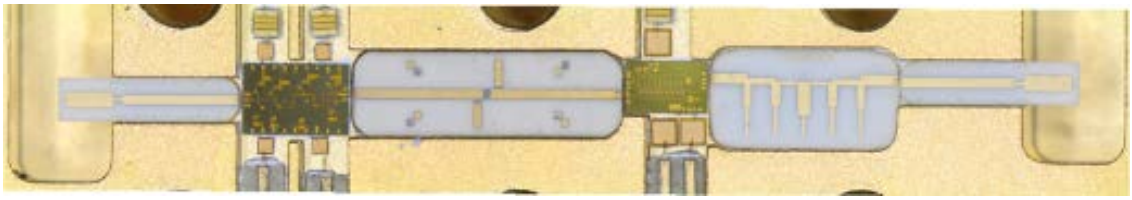

Figure 14. FGI BEM low-noise amplifier, internal view

7. PHASE SWITCHES

7.1 Thirty GHz Instrument Phase Switches

Phase switches module comprises two cascaded circuits, which individually introduces a relative phase difference of 90º and 180º. A driver integrated circuit (DR65-0109 from MACOM) controls phase states from appropriate TTL bias signals. The 90º phase switch uses single-pole double-throw (SPDT) switches and two microstrip band-pass filters (BPFs). SPDT is a combination of coplanar waveguide (CPW) and slotline transmission lines, in which microwave PIN diodes perform switching between paths. PIN diodes are connected in precise circuit positions.[6] The whole circuit uses 10-mils thick Alumina (A996) substrate. A picture of the 90º phase switch is in Figure 15.

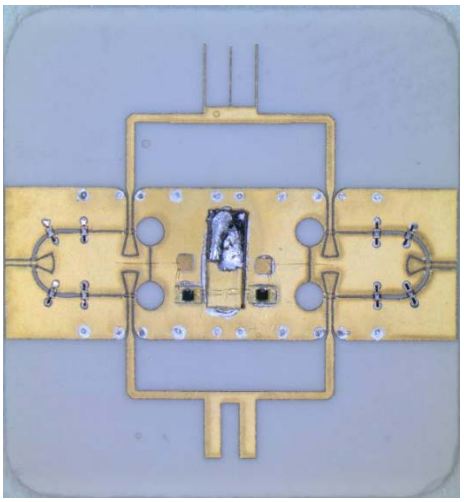

Figure 15. Picture of 90º phase switch for Thirty GHz Instrument

The 180º phase switch is a circuit based on coplanar waveguide (CPW) and slotline technologies, in which the phase shift is the phase difference of the electromagnetic waves feeding a CPW output line, transitioned from slotline. [7] The circuit uses also 10-mil thick Alumina (A996) substrate. In the slotline transmission path, there is a T-junction enabling to change the transmission path of the microwave signal, prior to CPW line transition. Transmission path selection is also done by microwave PIN diodes.

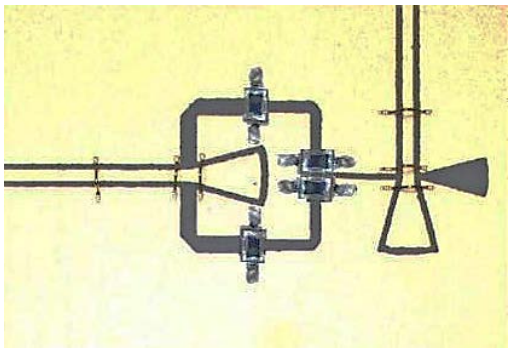

Figure 16. Picture of 180º phase switch for Thirty GHz Instrument

The combination of 90º and 180º phase switches performs four different phase states (0º, 90º, 180º and 270º). A picture of a branch of TGI Phase Switches Module is in Figure 17. Typical phase difference values of a representative unit, average from tests in 26 to 36 GHz band, are in Table 4.

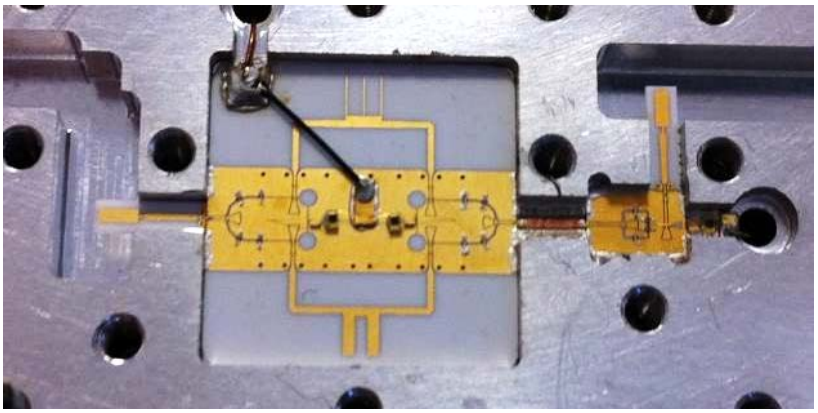

Figure 17. A phase switching branch of Phase Switches Module (TGI)

Table 4. Typical phase difference, average in 26-36 GHz band, for each branch (B1 or B2). Phase Switches Module TGI.

Phase switch state & Branch	Average value (º)
180º B1	179.4
90º B1	90.1
270º B1	271.8
180º B2	180.2
90º B2	90.7
270º B2	271.1

7.2 Forty GHz Instrument Phase Switches

The Phase Switches module has two separate and identical branches. Each branch has a microstrip circuit containing a power divider, a 180º phase switch, a fixed 90º differential phase shifter and a power combiner. This circuit introduces a relative phase difference of 90º, 180º and 270º by using TTL control signals. The switching devices are beam lead PIN diodes. Figure 18 shows a view of the phase switch and its equivalent block diagram.

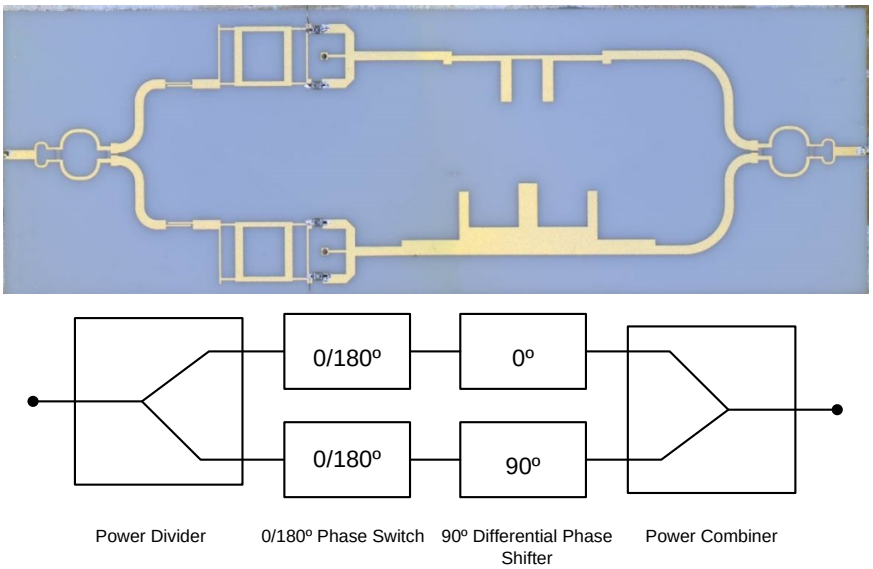

Figure 18. Phase switch microstrip circuit for Forty GHz Instrument and its equivalent block diagram.

The Phase Switch has four phase states (0º, 90º, 180º and 270º). Each phase state is the combination of the two independent 0º/180º phase switches states. At the power combiner output, the phase of the combined signal changes. Taken as 0º phase reference state when the two 0º/180º are in 0º state, then the phase difference introduced by the full circuit is 180º when both 180º phase switches are individually actuated, while when only one of 0º/180º phase switches, the upper or the lower, is actuated, then the phase difference is 90º or 270º.

Typical phase difference values of a Phase Switch branch in a representative unit, average from tests in 35 to 47 GHz band, are 88.8º, 178.7º and 272.3º. Experimental tests of a large amount of Phase Switches Modules show an almost identical phase response in both branches.

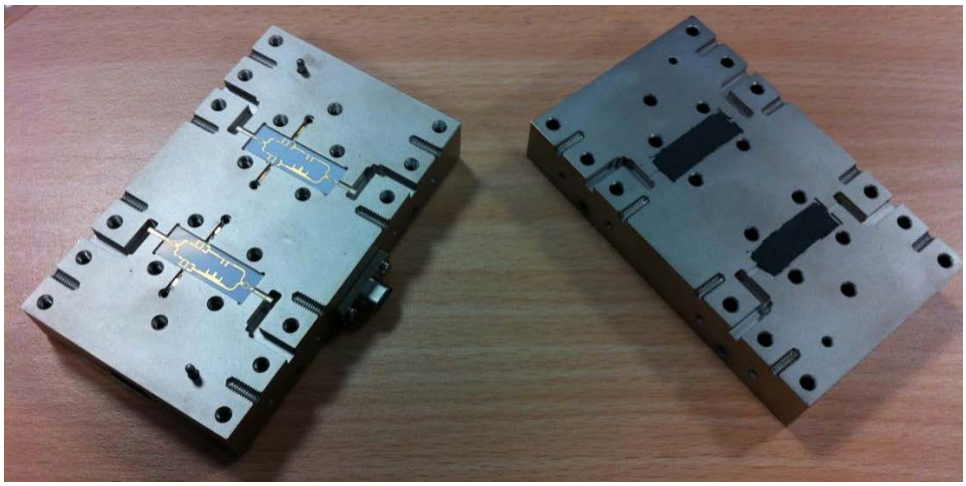

Figure 19. View of Phase Switches Module (FGI) opened.

8. CORRELATION AND DETECTION

8.1 Thirty GHz Instrument Correlation and Detection

Correlation and Detection subsystem in the TGI follows the scheme shown in Figure 3(a). Input signals are correlated by 180º broadband hybrids in microstrip lines technology. Figure 20 shows a picture of one of the hybrids within the module.

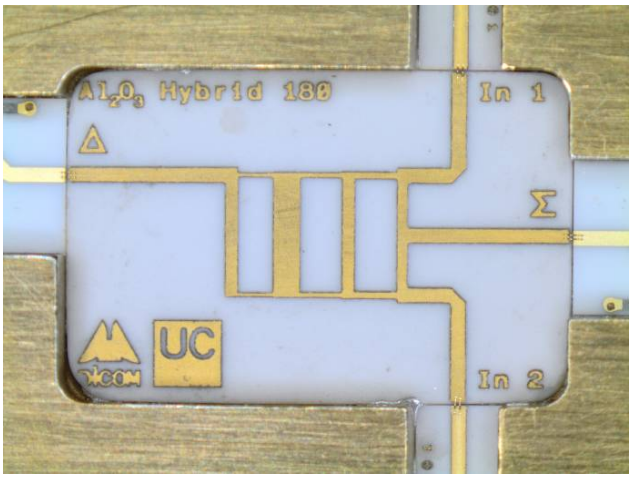

Figure 20. Broadband 180º microstrip hybrid for Correlation and Detection Module of TGI

Schottky diode detectors directly convert the microwave correlated signals to low frequency. Figure 21 shows a picture of one of these detectors.

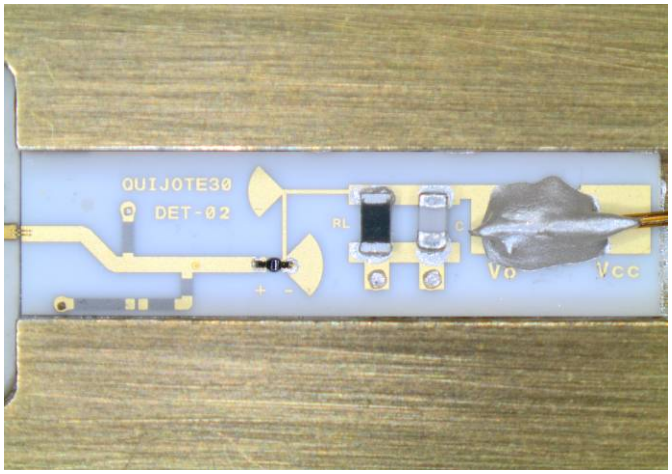

Figure 21. Schottky diode detector in Correlation and Detection Module (TGI)

Finally, the last subsystem within the Back-End Module is the DC amplifier. Each one of the four detectors outputs is amplified to accommodate their level to the desired voltage level at the data acquisition electronics (DAE) input. An open view of the TGI Correlation and Detection Module is in Figure 22; microwave correlator is on the left and DC amplifiers board is on the right.

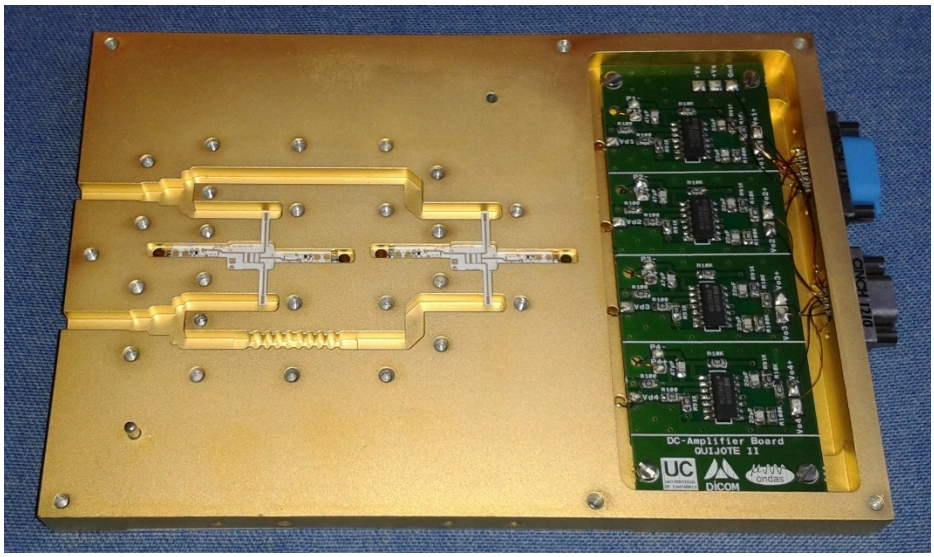

Figure 22. Correlation and Detection Module (TGI) open.

8.2 Forty GHz Instrument Correlation and Detection

This module consists of four 90º hybrid couplers, a 90º phase shifter and four Schottky diode detectors. Its block diagram scheme is in Figure 3(b). Low noise video amplifiers provide signal conditioning and low pass filtering. Hybrid couplers and 90º phase shifter are rectangular waveguide subsystems. Diode detectors are microstrip circuits. Waveguide components are built in two halves, Figure 23 shows both, being the rectangular waveguide cut in the E-plane. The four output detected voltages are amplified by low-noise DC amplifiers located in the module back side.

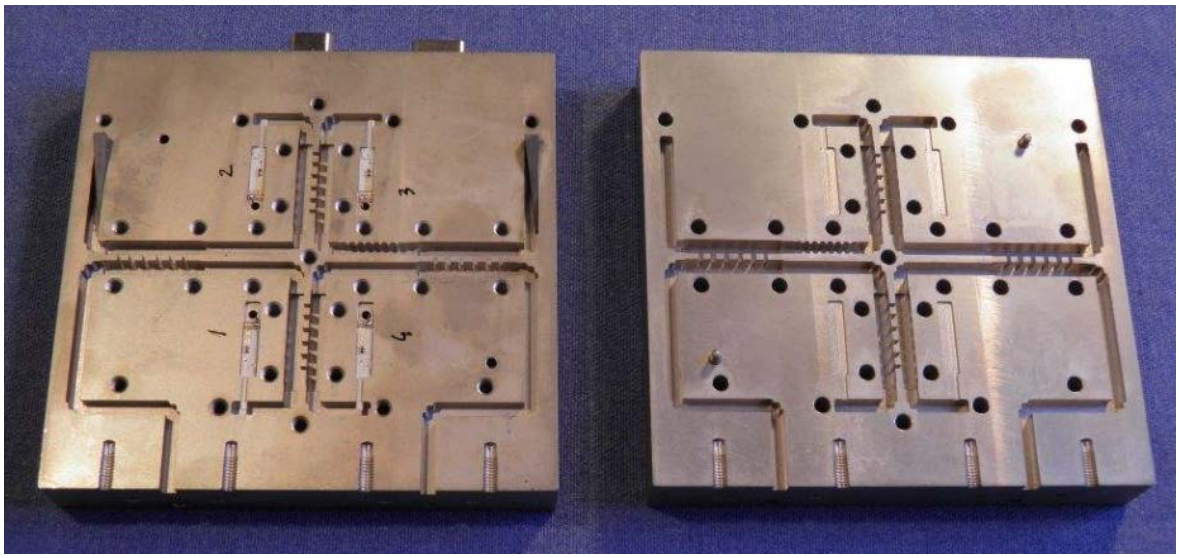

Figure 23. The two halves of Correlation and Detection Module (FGI).

9. BACK END MODULE RACKS

The installation of receivers in the telescopes requires the integration of several Back-End Modules, one per pixel, in standard 19 inches racks, containing all the mechanical and electrical interfaces for the appropriate operation of both instruments; Thirty and Forty GHz Instruments.

Thirty GHz Instrument has sixteen BEM pixels integrated per rack, in each BEM pixel there are three main separated subsystems: two RF Gain Modules, a Phase Switches Module and a Correlation-Detection Module. Figure 24 shows the assembly of these modules per pixel and the sixteen BEM pixels integrated in the rack. Input microwave interfaces are 2.92 mm (f) coaxial connectors. The TGI has two BEM racks containing 32 pixels in total.

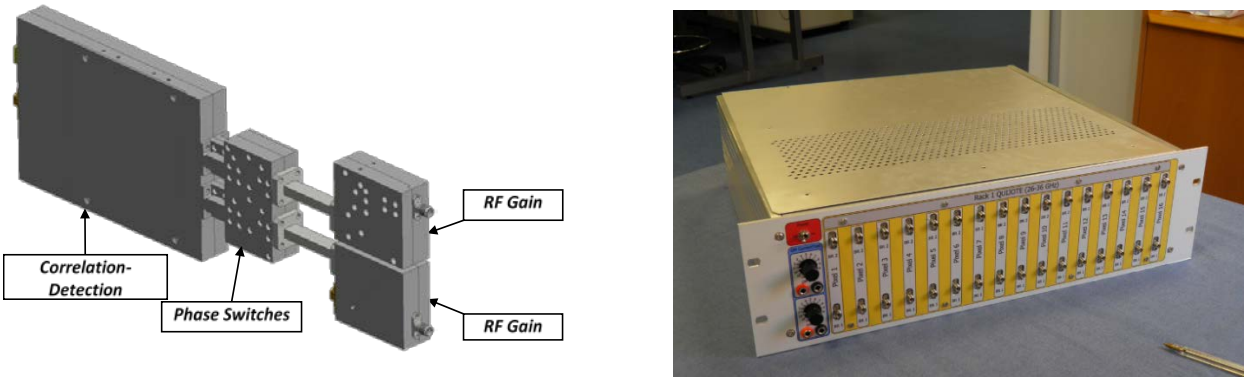

(a) (b)

Figure 24. Assembly of subsystems in TGI BEM: (a) One pixel, (b) Sixteen pixels rack.

Forty GHz Instrument has ten BEM pixels integrated per rack, in each BEM pixel there are also two Gain modules, a Phase Switches module and a Correlation-Detection module. Figure 25 shows the assembly of these modules per pixel and the ten BEM pixels integrated in the rack. Input microwave interfaces are WR22 rectangular waveguides with standard flanges. The FGI has three BEM racks containing 30 pixels in total.

For temperature control of all modules inside the rack, every pixel has attached a silicon heater mat and a temperature sensor. This temperature control permits the operation of all modules at a fixed temperature higher than ambient temperature at the observatory. The goal of this temperature control is to keep a fixed gain in the BEM along the time.

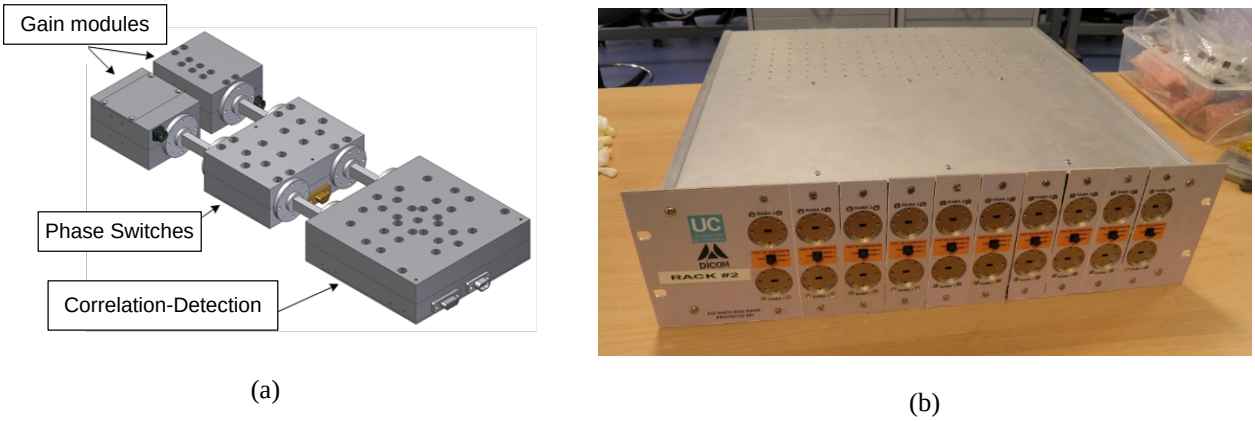

(a) (b)

Figure 25. Assembly of subsystems in FGI BEM: (a) One pixel, (b) Ten pixels rack.

The four output signals per pixel in both instruments, TGI and FGI, are the inputs for the Data Acquisition Electronics (DAE), for signal conditioning and data recording. The description of these subsystem is out of scope of the present paper.

10. CONCLUSION

The objective of this paper is the description of two broadband and low noise instruments, at 30 and 40 GHz, addressed to CMB polarization measurements. Each instrument has about 30 pixels and provides direct detection signals containing combinations of the Stokes parameters I, Q and U. Phase switching in the Back-End Module permits polarization modulation and gives redundant information to extract the Stokes parameters by reducing systematics effects. Each receiver has a cryogenic Front-End Module, to minimize the system noise temperature, followed by a room temperature Back-End Module performing microwave signals amplification, filtering, correlation and detection.

11. ACKNOWLEDGEMENT

The authors would like to thank Juan Luis Cano, José Vicente Terán, Jaime Cagigas and Angel Mediavilla for helping with the design and development of 30 and 40 GHz radiometer subsystems. They also would like to thank Eva María Cuerno and Ana Pérez for carrying the fabrication and assembly of passive and active subsystems of both receivers. The development of the TGI and FGI receivers has been funded by the Agencia Estatal de Investigación, Ministerio de Ciencia, Innovación y Universidades (Spain), and by the European Regional Development Fund (European Union).

REFERENCES

[1] M. R. Pérez-de-Taoro et alt. “QUIJOTE Experiment: status of telescopes and instrumentation”, Proc. SPIE 9906, Ground-based and Airborne Telescopes VI, 99061K (27 July 2016).

[2] F Poidevin, J A Rubiño-Martín, C Dickinson, R Génova-Santos, S Harper, R Rebolo, B Casaponsa, A Peláez-Santos, R Vignaga, F Guidi, B Ruiz-Granados, D Tramonte, F Vansyngel, M Ashdown, D Herranz, R Hoyland, A Lasenby, E Martínez-González, L Piccirillo, R A Watson, QUIJOTE scientific results – III. Microwave spectrum of intensity and polarization in the Taurus Molecular Cloud complex and L1527, Monthly Notices of the Royal Astronomical Society, Volume 486, Issue 1, June 2019, Pages 462–485, doi: 10.1093/mnras/sty3462

[3] A. Gomez, G. Murga, B. Etxeita, R. Sanquirce, R. Rebolo, J. A. Rubiño-Martin, J. M. Herreros, R. Hoyland, F. Gomez, R. T. Genova, L. Piccirillo, B. Maffei, R. Watson, "QUIJOTE telescope design and fabrication," Proc. SPIE 7733, Ground-based and Airborne Telescopes III, 77330Z (28 July 2010)

[4] E. Villa, J. L. Cano, J. Cagigas, D. Ortiz, F.J. Casas, A. R. Pérez, B. Aja, J.V. Terán, L. de la Fuente, E. Artal, R. Hoyland, A. Mediavilla, “The thirty gigahertz instrument receiver for the Q-U-I Joint Tenerife experiment: Concept and experimental results”, Review of Scientific Instruments 86, 024702 (2015)
[5] E. Villa, J. L. Cano, B. Aja, J.V. Terán, L. de la Fuente, A. Mediavilla, E. Artal, “Polarimetric receiver in the forty gigahertz band: new instrument for the Q-U-I joint Tenerife experiment”. Experimental Astronomy (2018) 45:127–146
[6] E. Villa, B. Aja, J. Cagigas, L. de la Fuente, E. Artal, “Design methodology and performance analysis of a wideband 90° phase switch for radiometer applications”, Review of Scientific Instruments 84, 124704 (2013); doi: 10.1063/1.4849555
[7] E. Villa, B. Aja, J. L. Cano, L. de la Fuente and E. Artal, "Cryogenic Ka-Band 180º Phase Switch Based on Schottky Diodes," in IEEE Microwave and Wireless Components Letters, vol. 22, no. 2, pp. 52-54, Feb. 2012, doi: 10.1109/LMWC.2011.2179920.